

Heat capacity and high-resolution Brillouin scattering studies of phase transitions in $\text{K}_2\text{MgWO}_2(\text{PO}_4)_2$: Observation of the coupled soft optic and acoustic mode

M. Mączka and J. Hanuza

Institute of Low Temperature and Structure Research, Polish Academy of Sciences, P.O. Box 1410, 50-950 Wrocław 2, Poland

A. Majchrowski

Institute of Applied Physics, Military University of Technology, 2 Kaliskiego Street, 00-908 Warszawa, Poland

S. Kojima

Institute of Materials Science, University of Tsukuba, Tsukuba, Ibaraki 305-8573, Japan

(Received 19 February 2007; published 7 June 2007)

High-resolution micro-Brillouin scattering and heat capacity studies of phase transitions in ferroelectric $\text{K}_2\text{MgWO}_2(\text{PO}_4)_2$ were performed in the temperature range 300–810 K. Strong anomalies in Brillouin shift and attenuation were observed near 633, 519, and 434 K upon cooling for the sound waves corresponding to the c_{11} and c_{33} elastic constants. The analysis of these anomalies and heat capacity results revealed that they correspond to second-order, typical first-order, and nearly second-order phase transitions, respectively. The highest temperature phase transition was shown to have mainly an order-disorder nature whereas the two remaining transitions may have both order-disorder and displacive nature. The obtained results revealed also very strong coupling between the c_{44} acoustic mode and the soft optic mode of E symmetry. The coupled mode model was employed to fit the experimental data. It was shown that the relaxation time of the order parameter exhibits slowing down indicating that the phase transition at 519 K is induced by instability of the E -symmetry soft mode. The possible microscopic origin of the soft mode is proposed.

DOI: [10.1103/PhysRevB.75.214105](https://doi.org/10.1103/PhysRevB.75.214105)

PACS number(s): 78.35.+c, 65.40.Ba, 62.20.Dc, 77.80.Bh

I. INTRODUCTION

One of the most outstanding and widely used nonlinear-optical phosphates is KTiOPO_4 (KTP).^{1,2} KTP undergoes a second-order displacive-type structural phase transition at 1206 K from the high-temperature paraelectric $Pnan$ phase to a low-temperature ferroelectric $Pna2_1$ phase.³ It was reported that the K^+ cation and the TiO_6 octahedron both play a significant role in this transition.⁴ A soft optical mode was observed but its temperature dependence was complicated due to a coupling to a relaxation mode.^{4,5} Temperature-dependent Brillouin studies were performed only for longitudinal acoustic (LA) modes.^{6,7} They revealed clear but relatively weak acoustic anomalies at T_c . It was also reported that the mechanism of the phase transition and nonlinear properties are greatly changed if K^+ (Ti^{4+}) ions are replaced by other cations such as Rb^+ , Cs^+ , Tl^+ (Zr^{4+} , Sn^{4+} , Ge^{4+}).^{1,4,8} For instance, replacement of K^+ by Tl^+ ions led to the appearance of a very clear soft mode typical for a displacive transition,⁴ whereas the second-order phase transition in germanate analogs of KTP was shown to be both displacive and order-disorder in nature.⁸

$\text{K}_2\text{MgWO}_2(\text{PO}_4)_2$ (KMWP) is derived from KTP by replacement of two Ti^{4+} ions with Mg^{2+} and W^{6+} cations.^{9–11} The replacement of titanium ions leads to significant changes in the structure and phase transition sequence. First, the high-temperature structure is tetragonal, with the space group $P4_12_12$. Second, the polymorphism of this crystal is much richer than that of KTP. The previous data scanning calorimetry (DSC), ionic conductivity and dielectric studies showed that KMWP undergoes successive structural transitions at $T_3=537$, $T_2=535$, and $T_1=436$ K from the $P4_12_12$ tetragonal

phase into the $P2_12_12_1$ orthorhombic, $P2_1$ monoclinic, and $P1$ triclinic phases.^{9–11} Below 537 K KMWP displays ferroelastic properties, and below 535 K, in addition, ferroelectric properties.^{9–11} The previous studies showed also that KMWP undergoes two additional phase transitions at $T_4=637$ and $T_5=782$ K. It was suggested that these transitions occur without any alternation of the tetragonal symmetry.^{9–11} We would like to emphasize, however, that the crystal structure of KMWP was determined only at 773 K and room temperatures.^{9–11} Therefore symmetries of the phases observed in the 436–535 K (denoted in the further discussion as phase II), 535–537 K (phase III), and 537–637 K temperature ranges (phase IV) as well as above 782 K (phase VI) are still uncertain, and the mechanisms of the phase transitions have not been understood up to now.

Recently a discovery of two central peaks in KMWP was reported by us.¹² The present paper is devoted to heat capacity studies and studies of acoustic properties of KMWP in a very broad temperature range, 300–810 K. It will be shown that heat capacity and Brillouin scattering give new information, which significantly contributes to understanding of the phase transition mechanisms in this compound. In particular, our results reveal the presence of the soft-optic and acoustic mode coupling phenomenon.

II. EXPERIMENT

$\text{K}_2\text{MgWO}_2(\text{PO}_4)_2$ (KMWP) crystals were obtained from K_2WO_4 - WO_3 flux ($\text{K}_2\text{WO}_4/\text{WO}_3$ molar ratio 0.53/0.47) according to work of Peuchert *et al.*¹⁰ The starting melt contained the stoichiometric mixture of KH_2PO_4 , MgO and WO_3 corresponding to the KMWP compound and the potas-

sium tungstate flux in the molar ratio equal to 2.5/1 (compound/flux). The synthesis of the melt was done directly in the platinum crucible 30 mm in height and diameter from which the crystallization was carried out under conditions of low temperature gradients. After soaking the melt at 795 °C for 24 h, it was cooled down at the rate of 0.2 °C/h for 14 days and then it was cooled down to room temperature at the rate of 20 °C/h. KMWP crystals were extracted from the solidified melt by its dissolution in water.

Heat capacity was measured using the Thermal Analyst 2000 calorimeter (TA Instruments). The sample mass was of the order of 15 mg. The measurements were made for a modulation frequency of 10 mHz and peak-to-peak temperature modulation amplitude of 1 K. The sample was heated at 2 K/min from 373 to 823 K and then cooled down to 373 K.

The Brillouin spectra were obtained with a 3+3 pass tandem Sandercock-type Fabry-Perot interferometer combined with an optical microscope. The free spectral range (FSR) of 44 GHz was employed. The scattered light from the sample was collected in the back-scattering geometry. An additional measurement in 90° scattering geometry was performed only at room temperature in order to obtain information about refractive indices. A conventional photon-counting system and a multichannel analyzer were used to detect and average the signal. The samples were put in a cryostat cell (THMS 600). The sample cell with X-Y adjustment was placed onto the stage of an optical microscope (Olympus BH-2) having Z-adjustment. The Brillouin spectra were obtained for 1024 channels after 500 time repetitions of accumulation with a gate time of 500 ms for one channel. More details of the experimental setup can be found in our previous paper.¹³

The frequency shifts, half-widths, and intensity of the Brillouin peaks corresponding to longitudinal acoustic (LA) modes were evaluated by fitting the measured spectra to the convolution of the Gaussian instrumental function with a theoretical spectral line shape that is Lorentzian in form.¹⁴ Analysis of the coupled optic and transverse acoustic (TA) mode was performed in a way proposed by Reese *et al.*¹⁵ (see discussion section). Sound velocities and corresponding elastic constants were calculated from the measured frequency shifts using the mass density $3.69 \times 10^3 \text{ kg/m}^3$. The refractive indices $n_o=1.69$ and $n_e=1.70$ were obtained by comparing measurements of Brillouin shifts in backscattering and 90° configuration in the way proposed by Vaughan.¹⁶

III. RESULTS AND DISCUSSION

A. Heat capacity

The heat capacity versus temperature is presented in Fig. 1(a). Clear anomalies are observed upon cooling near 633, 519, and 434 K, which can be attributed to T_4 , T_2 , and T_1 , respectively. No heat capacity anomaly could be found around T_5 and T_3 . In order to determine the phase transition temperatures and the thermodynamic quantities associated with the phase transitions, we needed to separate the excess heat capacity due to the phase transition from the lattice heat capacity. The dashed line in Fig. 1(a) represents the lattice heat capacity estimated by fitting the experimental data with

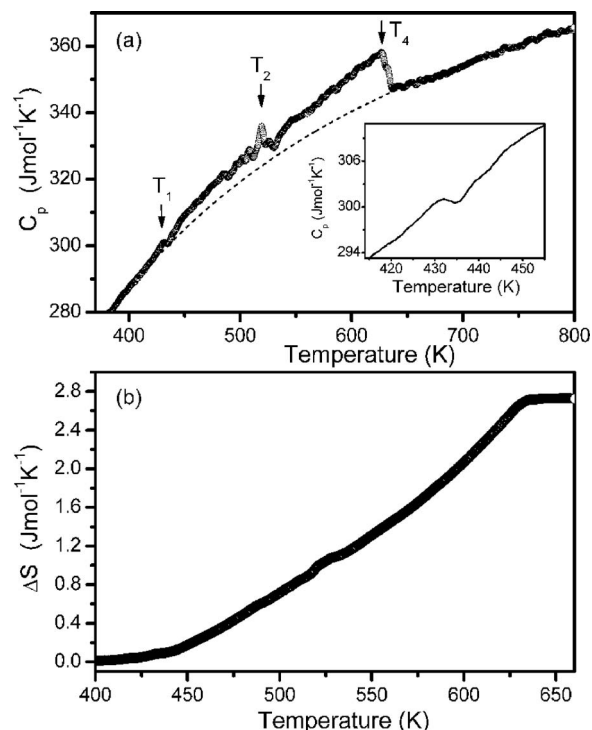


FIG. 1. (a) Heat capacity of KMWP measured during a cooling run (open circles). The dashed line shows the lattice heat capacity. The inset shows details near T_1 . (b) Excess entropy in KMWP.

single Debye and Einstein functions. Three Einstein functions were chosen since our Raman studies show that the Raman spectra (not shown in the present paper) consist of three spectral ranges: 56–428, 510–629, and 826–1192 cm^{-1} . Einstein temperatures (355, 823, and 1439 K) were estimated from the average Raman frequencies calculated for every of the three spectral ranges. As can be noted in Fig. 1(a) the fit is rather good with the Debye temperature 274 K. It should be noted, however, that the obtained Einstein and Debye temperatures are only approximate since the ir frequencies were not included in the estimation of Einstein temperatures. Nevertheless, the evaluation of the background is quite reasonable and its subtracting from the experimental heat capacity and integrating of $(\Delta C_p/T)dT$ gives estimation of the excess entropy [see Fig. 1(b)].

The heat capacity data show a jump increase at $T_4 = 632.6 \pm 0.1 \text{ K}$ with $\Delta C_p = 13.5 \pm 0.1 \text{ J mol}^{-1} \text{ K}^{-1}$. The shape of the observed anomaly and the fact that no sign of thermal hysteresis across this transition was observed indicate that the transition is second-order or very close to second-order. The temperature of this anomaly is nearly 5 K lower in comparison with the 637 K value reported in literature.^{9–11} This difference may most likely be related to a small difference in potassium stoichiometry of the studied here and previously studied crystals, since the former studies of KTP showed that the phase transition temperature in this class of materials may change slightly, depending on the potassium stoichiometry.¹⁷ The temperature dependence of the excess entropy ΔS is nearly linear, as expected for a second-order phase transition. The transition entropy $2.7 \text{ J mol}^{-1} \text{ K}^{-1}$ is

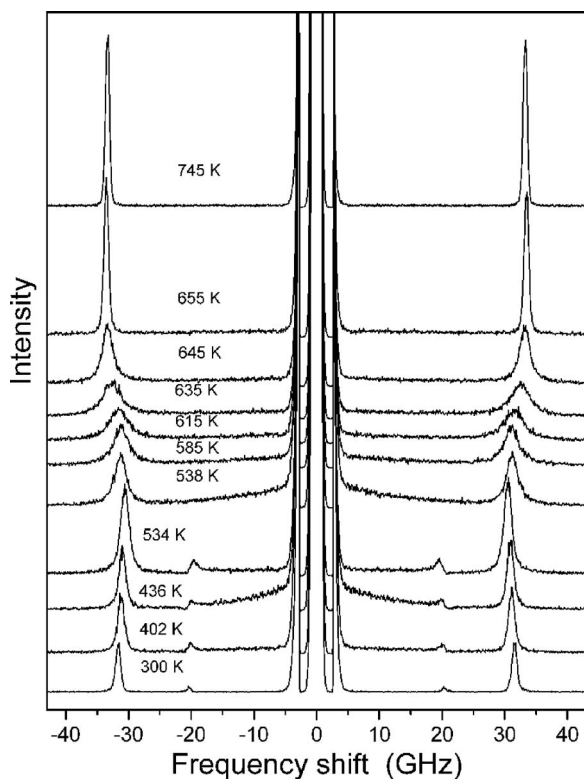


FIG. 2. Example of the temperature dependence of the $y(xx+xz)-y$ Brillouin spectra for KMWP.

only about 47% of $R \ln 2 = 5.7 \text{ J mol}^{-1} \text{ K}^{-1}$, where R is the gas constant, which is expected for a typical order-disorder phase transition in systems consisting of two states per particle. It is, however, higher than the $0.2407R$ value found for KD_2PO_4 (DKDP), undergoing a phase transition which is both displacive and order-disorder in nature.¹⁷ This result suggests that the phase transition at T_4 in KMWP may also be both displacive and order-disorder in nature, similarly as observed for DKDP,¹⁸ as well as germanate analogs of KTP.⁸

The two remaining heat capacity anomalies, observed at $T_2 = 519.1$ and $T_1 = 433.6$ K, are characterized by 0.18 and about $0.1 \text{ J mol}^{-1} \text{ K}^{-1}$ transition entropies. The nearly symmetric shape of the anomaly observed near T_2 and the fact that this anomaly exhibits large thermal hysteresis of 14.8 K indicates that this is a first-order phase transition. On the other hand, no thermal hysteresis can be observed for the phase transition at T_1 . Moreover, the shape of the heat capacity anomaly at T_1 is similar to that observed at T_4 . These facts indicate that the phase transition at T_1 is the second-order or close to the second-order one.

B. Temperature dependence of longitudinal acoustic phonons

Typical Brillouin spectra from KMWP for $y(xx+xz)-y$ scattering geometry are shown in Fig. 2, where y , x , and z correspond to the b , a , and c tetragonal axes, respectively. In this scattering geometry only one peak is observed at high temperatures which can be assigned to the longitudinal acoustic (LA) mode corresponding to the c_{11} elastic constant. This observation is in agreement with the $P4_12_12$

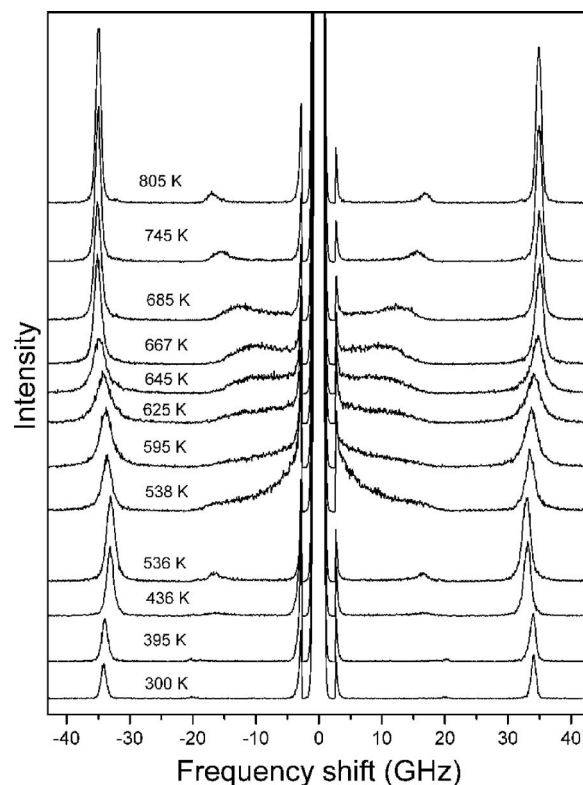


FIG. 3. A few typical Brillouin spectra for approximately $z(xx+xy)-z$ scattering geometry (incident and scattered light deviates about 5° from the z axis).

symmetry.¹⁹ Figure 3 shows typical Brillouin spectra for phonons traveling nearly parallel to the z axis. The deviation from the z axis, about 5° , was used in order to monitor temperature dependence of both LA and TA modes, corresponding to the c_{33} and c_{44} elastic constants, respectively [for the pure $z(xx+xy)-z$ scattering geometry the TA mode could not be observed in the tetragonal phase]. Using the obtained data we were able to estimate c_{11} , c_{33} , and c_{44} elastic constant at 800 K as 100.8, 111.5, and 36.2 GPa, respectively. These values are significantly smaller than the corresponding values in KTP, which are $c_{11} = 166$, $c_{33} = 181$, and $c_{44} = 56$ GPa.⁶

The plots of frequency and damping for LA modes versus temperature, presented in Fig. 4, show no anomalies around T_3 and T_5 . This result is consistent with the heat capacity studies, which also did not show any anomalies at these temperatures. On the other hand, distinct acoustic anomalies occurred near T_1 , T_2 , and T_4 . At T_4 , frequencies of the LA modes exhibit downward steps and the Brillouin linewidths exhibit maxima approximately in the middle of the downward steps. This type of behavior shows that a dominant contribution to the observed acoustic anomalies of LA modes is related to the Landau-Khalatnikov mechanism, i.e., the LA acoustic modes couple with the square of the order parameter.^{20,21} This observation gives also strong evidence that disorder processes play a major role in this phase transition. It is to be noted that the observed anomalies extend over a very broad temperature range, in agreement with the heat capacity results. At T_2 , the LA mode traveling along the y axis splits into two components [see Fig. 4(b)], which can

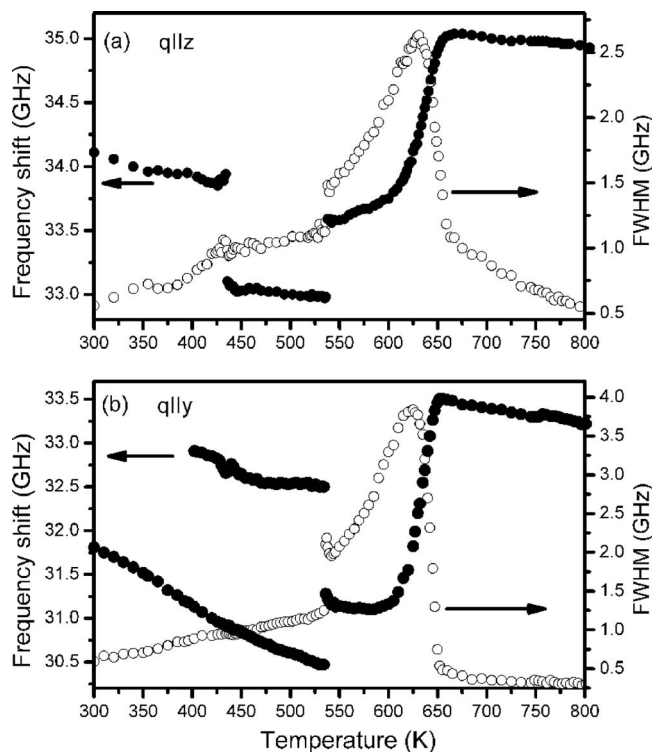


FIG. 4. Temperature dependence of frequency shift (closed circles) and the corresponding full width at half maximum (open circles) for a longitudinal phonon propagating in a direction parallel to the z axis (a) and parallel to the y axis (b).

be observed separately in different experimental runs due to the application of the microscope in the present studies. This splitting indicates that the LA phonons traveling along x and y axes have no longer the same frequency below T_2 and the crystal is composed of ferroelastic domains below T_2 . This observation is in agreement with the monoclinic symmetry, suggested by Peuchert *et al.*^{9–11} The phase transition at T_2 also leads to a jump frequency decrease of the LA phonon traveling along the tetragonal z axis. Another characteristic feature is a jump decrease of the acoustic modes damping. The phase transition at T_1 leads to very weak anomalies in the frequency of the LA phonons traveling along the tetragonal y axis but a clear jump is observed for the phonon traveling along the z axis. The anomalies in damping are very weak but it is obvious from Fig. 4 that damping does not show a jump decrease, like at the T_2 transition. The shape of the observed anomalies near T_2 and T_1 indicates that they are caused by coupling of the LA modes to the square of the order parameter. Different behavior of damping near T_1 and T_2 is consistent with our heat capacity results, which have revealed strongly the first-order nature of the phase transition at T_2 and second-order or close to the second-order nature of the phase transition near T_1 .

The observed anomalies around T_4 can be analyzed to obtain information on the relaxation of the order parameter in phase IV. We have attempted to extract the relaxation time from the temperature dependence of the c_{22} mode only since in this case a contribution to the observed anomaly from the coupling between the LA mode and square of the order pa-

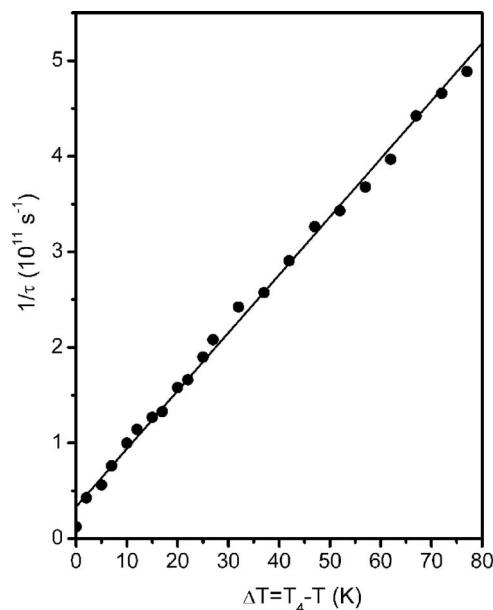


FIG. 5. Temperature dependence of inverse relaxation time in phase IV for a LA phonon propagating parallel to the y axis.

rameter fluctuations seems to be negligible. Assuming that the single relaxation time, τ , is appropriate, it can be determined from the relation^{21,22}

$$\frac{1}{2\pi\tau} = \frac{\nu_\infty^2 - \nu_0^2}{\Gamma_0 - \Gamma_\infty}. \quad (1)$$

Here ν_∞ (Γ_∞) is the observed Brillouin shift (linewidth) and ν_0 (Γ_0) is the Brillouin shift (linewidth) not affected by the transition. The Brillouin linewidth observed far above T_4 (0.36 GHz) was taken as Γ_0 . In order to evaluate ν_0 , the experimental data in the 650–740 K temperature range were fit to a linear function. The best fit yielded $\nu_0 = 34.90 - 0.00212T$ and this formula was used to obtain ν_0 below T_4 . The plot of $1/\tau$ obtained from the experimental data for the c_{22} mode with Eq. (1) is shown in Fig. 5. As it can be seen $1/\tau$ is approximately a linear function of temperature, in good agreement with the Landau theory.²³ Such behavior is known as a “critical slowing down” where $1/\tau$ can be described by the formula^{24,25}

$$\frac{1}{\tau} = \frac{T_4 - T}{T_4} \frac{1}{\tau_0} + \frac{1}{\tau_1}. \quad (2)$$

Best fit to the experimental data with Eq. (2) yields $\tau_0 = 0.26$ ps and $\tau_1 = 30.1$ ps. The relaxation time in KMWP is of similar order of magnitude as the relaxation times observed for typical order-disorder ferroelectrics. For instance, τ_0 is 0.12 ps for KH_2PO_4 (KDP),²⁶ and 0.096 ps for triglycine sulfate (TGS).²⁷

C. Temperature dependence of the transverse modes: Coupled optic and acoustic mode phenomena

Figure 2 shows that no transverse mode is observed above 538 K temperature in $y(xx+xz)-y$ configuration. When,

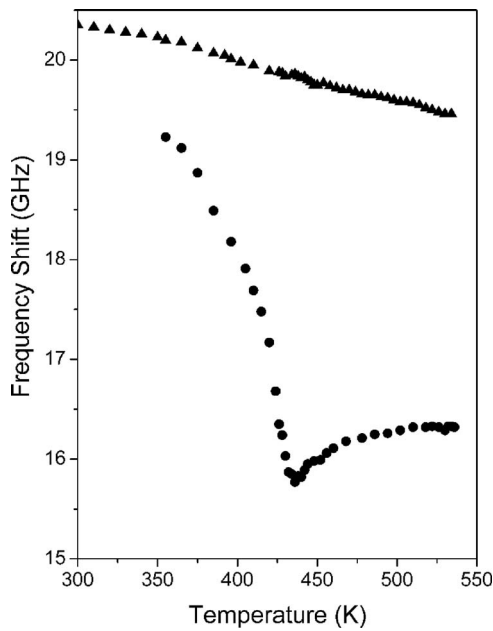


FIG. 6. Temperature dependence of a frequency shift for a quasitransverse mode propagating along the y axis (triangles) and a transverse mode propagating along the z axis (circles).

however, the temperature is lowered below 538 K, a transverse acoustic mode appears. In the monoclinic phase, for light propagating along the polar C_2 axis, the two transverse modes are forbidden.¹⁹ For propagation along the axis perpendicular to the C_2 axis, within the xy -plane of the tetragonal phase, there exists only one purely transverse mode, c_{66} , which is allowed when the incident and scattered beams are polarized perpendicularly to each other.¹⁹ The two remaining modes, quasilongitudinal and quasitransverse, are allowed with parallel polarizations.²⁸ Since the mode near 20 GHz is observed only for parallel polarizations in the 436–536 K temperature range,¹² it can be attributed to the quasitransverse mode. It corresponds to the c_{44} mode in the tetragonal phase and is related in the monoclinic phase to²⁸

$$c_{55} + \frac{c_{51}^2}{c_{11} - c_{55}}. \quad (3)$$

Our results show that frequency shift of this mode exhibits no clear anomaly at T_1 (see Fig. 6).

Figure 7 shows that the TA phonon propagating nearly parallel to z axis (corresponding to c_{44} elastic constant) exhibits a strongly asymmetric shape already at 810 K. The frequency of this mode decreases, and damping and intensity increase significantly when the temperature decreases. This behavior resembles very much temperature dependence of the coupled soft optic and acoustic modes observed previously in hexagonal BaTiO_3 and orthorhombic DKDP.^{15,29–32} However, in contrast to DKDP and hexagonal BaTiO_3 , for which the coupled mode features are observed in a narrow (less than 30 K) temperature range, KMWP exhibits coupled mode features in a very broad temperature range (about 250 K). It should be noted that the c_{44} mode splits below T_2 into two components. One component is observed near

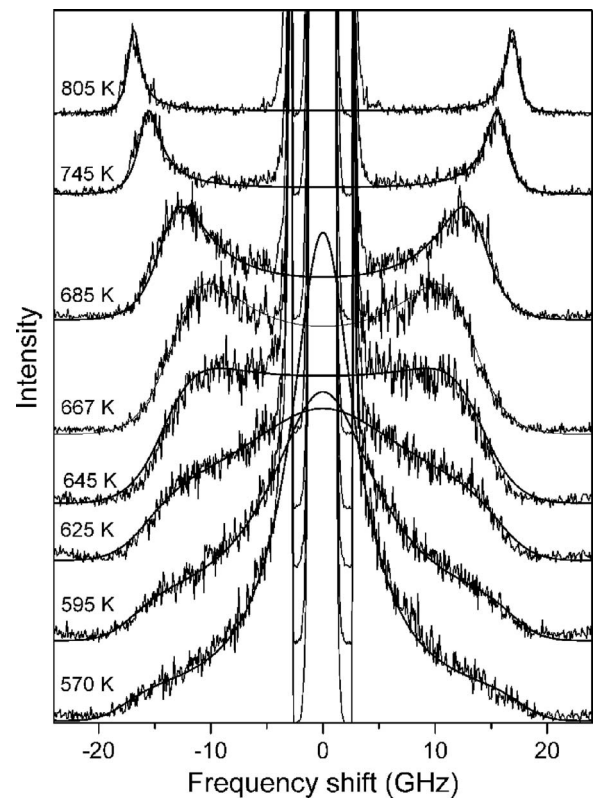


FIG. 7. Typical $z(xx+xy)-z$ spectra showing the coupled optic and acoustic mode. The solid lines, presented only for the tetragonal phase, are theoretical spectra calculated with the model developed by Reese *et al.* (Ref. 15).

20 GHz as a very weak and narrow band whereas the second component is observed near 16 GHz as a strongly asymmetric band. This result indicates that the lower frequency component couples significantly to the soft mode. According to the selection rules, in this scattering geometry the purely transverse mode corresponds to c_{44} elastic constant and is related to B -symmetry excitation. The quasitransverse, A -symmetry mode, is related to²⁸

$$c_{55} + \frac{c_{53}^2}{c_{33} - c_{55}}. \quad (4)$$

The comparison of the spectra allows us to assign the Brillouin peaks near 20 and 16 GHz to the quasitransverse and transverse mode, respectively. This result shows that the coupling is observed only for the B -symmetry modes. When temperature decreases, the frequency of this coupled c_{44} mode decreases slightly when T_1 is approached from above (see Fig. 6). Below T_1 , the frequency of this mode increases and its intensity significantly decreases. These features indicate that the coupling strength decreases in the triclinic phase with decreasing temperature.

Let us now analyze the observed coupled modes. According to selection rules, the c_{44} phonon of phase V (space group $P4_12_12$, point group D_4) is allowed to couple bilinearly only with the optic mode of E symmetry. This optic mode is polar, therefore the observed coupling can be described as piezoelectric. Since the acoustic mode we ob-

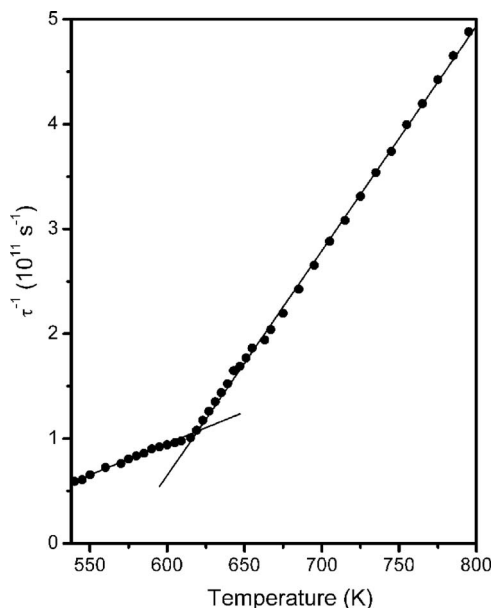


FIG. 8. Temperature dependence of inverse relaxation time $1/\tau$ estimated from the temperature dependence of the coupled transverse mode.

served is a purely shear, described by x_4 strain, the relevant coupling term is $a_{14}P_1x_4$, where a_{14} is the piezoelectric constant and P_1 is polarization. The equations of motion for the coupled acoustic and optic mode, propagating in the direction of wave vector q , can be written in terms of the strain x and polarization P :

$$(\omega_0^2 - \omega^2 - 2i\omega\Gamma_0)P - (a/m)x = E/m, \quad (5)$$

$$(-a/\rho)P + (\omega_a^2 - \omega^2 - 2i\omega\Gamma_a)/q^2x = \sigma/\rho, \quad (6)$$

where Γ_0 (Γ_a) and ω_0 (ω_a) are the optic (acoustic) damping and frequency; m , ρ , E , and σ are the effective mass of the E mode, density, the force conjugated to P , and stress, respectively. The solution of Eqs. (5) and (6) yields the susceptibility $\chi(\omega)$ which gives information about the scattered spectrum. Details of the derivation can be found in Ref. 15.

In Fig. 7 the theoretical curves are presented together with the experimental data. These theoretical curves were fitted to the experimental spectra using the model presented by Reese *et al.* in Ref. 15. It can be noticed that the spectra are fitted very well in the framework of the coupled-mode model. This result gives evidence that the coupled-mode model is an adequate theoretical model for describing the temperature dependence of the observed mode. Since the soft optic mode gives a rise to a central peaklike feature below T_4 , it is clear that this mode is strongly overdamped. The former studies of hexagonal BaTiO₃ showed that ω_0 alone is not a feasible quantity to specify the state of the soft mode near the phase transition when it is strongly overdamped.²⁹ Instead, a ratio of the square of the soft mode frequency and the damping constant, ω_0^2/Γ_0 , should be considered since this ratio corresponds to $1/2\pi\tau$. Figure 8 presents the temperature dependence of $1/\tau$ obtained from the best fit. According to this figure $1/\tau$ shows a linear dependence on temperature both in

phases V and IV. This result indicates that critical slowing down is observed in a broad temperature range. There is, however, a distinct change in the slope of $1/\tau$ vs temperature around 620 K temperature, i.e., about 12 K below T_4 . This temperature correlates well with the maximum of the dielectric anomaly, which was observed near 621 K.⁹ Assuming critical behavior of τ , the data were fit to the relation

$$\frac{1}{\tau} = \frac{|T - T_0|}{T_0} \frac{1}{\tau_0}. \quad (7)$$

The least-squares analysis with Eq. (7) gave $\tau_0=0.82$ ps and $T_0=568.9$ K for phase V and $\tau_0=3.8$ ps and $T_0=440.7$ K for phase IV. It should be noted that the relaxation time τ_0 is significantly longer than that typically observed for order-disorder phase transitions. For instance, in the ferroelectric phases of PbHPO₄, TGS, and nearly stoichiometric LiTaO₃, τ_0 was found to be 0.04, 0.096, and 0.014 ps, respectively.^{27,33,34} Similar time as for KMWP was found, however, for DKDP (1.3 ps in the piezoelectric tetragonal phase¹⁵), which is known to exhibit a phase transition of both order-disorder and displacive type.³⁵

The coupling of the soft optic and the c_{44} acoustic mode is much weaker in the monoclinic and triclinic phases than in the tetragonal phase. As a result, the intensity of the observed Brillouin peak is weak and fitting of the spectra with the coupled mode model is not very reliable.

D. Mechanism of the phase transitions and microscopic origin of the relaxation mode

It was previously suggested that the phase transition at T_4 occurs either without any alternation of KMWP's tetragonal symmetry, i.e., the phase transition is isosymmetric, or the phase IV is modulated.⁹⁻¹¹ Present Brillouin results show that the c_{11} and c_{33} modes, transforming according to the A_1 irreducible representation of the D_4 point group, do not couple to the order parameter in phase V but they couple in phase IV. This means that the lowest-order coupling of strain x to the order parameter η allowed by symmetry has the form $1/2x\eta^2$. This result shows that the phase transition at T_4 in KMWP is not isosymmetric since such a transition must be governed by the order parameter that transforms according to the same irreducible representation both below and above the phase transition temperature.³⁶ The Brillouin results could be, however, explained assuming that the transition into tetragonal modulated or incommensurate structure occurs. We may also assume that the transformation is induced by a Brillouin zone center instability transforming according to the representation A_2 of the higher-temperature D_4 phase. In this case the point symmetry would change from D_4 to C_4 and bilinear coupling of strain to the order parameter of A_2 -symmetry would be forbidden. Symmetry change from D_4 to C_4 is consistent with the temperature dependence of dielectric constant that showed a pronounced peak at T_4 mainly for ϵ_{33} .⁹ Since the C_4 group is polar, the transition could be classified as ferroelectric and the temperature dependence of the relaxation time, shown in Fig. 5, would correspond to relaxation of the polarization P_3 . As it can be seen in Fig. 4, the broad anomaly in damping is observed for the

both LA modes traveling along the z and y axes. If we assume C_4 symmetry below T_4 , this result would indicate that the damping anomaly is observed even for the phonon traveling parallel to spontaneous polarization P_3 (q parallel to the z axis). It is well-known that the fluctuation of electric polarization ΔP shows a characteristic anisotropy near T_c owing to the long range electrostatic dipole-dipole interaction.^{37,38} The longitudinal component of ΔP is suppressed by the appearance of the depolarization field, while the transverse one is not.^{37,38} This anisotropy can be observed in Brillouin studies for those phonons which are allowed to couple bilinearly with ΔP below T_c : if a phonon propagates along q , Brillouin spectra usually do not show any anomaly in damping because of the suppressed fluctuation.^{33,39} If q is perpendicular to P , strong anomaly in damping is predicted to be observed.^{33,39} It should be noted, however, that for weak ferroelectrics and for some crystals exhibiting high ionic mobility significant acoustic anomalies can be observed even if q is parallel to P .^{40,41} Since ionic conductivity in phase IV is very large, the observed behavior of the LA phonon traveling along the z axis could be explained by the increase in the ionic mobility in this phase.

The above discussion shows that the observed Brillouin anomalies do not give an unambiguous answer regarding symmetry of phase IV. Although a number of observations indicate that KMWP may undergo at T_4 a phase transition from D_4 into the C_4 phase, this symmetry change should also lead to the appearance of transverse modes below T_4 , which were, however, not observed. On the other hand, a transition into modulated structure seems to be not consistent with x-ray studies, which revealed the same number of formula units both at the high-temperature tetragonal phase and room-temperature triclinic phase.^{10,11} We cannot, however, exclude the possibility that the phase transition at T_4 is a cell-multiplying transition and then the smaller room-temperature unit cell is obtained as a result of the phase transition at T_1 or T_2 . It should be also noted that the observation of an unusually broad acoustic anomaly below T_4 may favor the conclusion that the intermediate phase IV is incommensurate.

Very strong coupling between the c_{44} acoustic mode and the optic mode of E -symmetry in the tetragonal phases indicates that the phase transition at T_2 is triggered by instability of this Brillouin zone center mode. It was shown previously that in case of coupling between an optic and acoustic mode, the phase transition occurs when the frequency of the coupled optic-acoustic mode drops to zero.¹⁵ However, the frequency of the optic mode will take a finite value at the phase transition.¹⁵ Our results show, therefore, that the phase transition at T_2 can be classified as primary ferroelastic. As a result of this transition, the E -symmetry soft optic mode should split in the monoclinic phase into two components of A - and B -symmetry. Since we do not observe any coupling between the A -symmetry optic mode and the quasitransverse acoustic modes, frequency of the optic mode is probably well above 20 GHz. On the other hand, significant coupling between the B -symmetry mode indicates that frequency of the B -symmetry soft optic mode is still relatively small.

The transition at T_1 is certainly not driven by instability of the c_{44} transverse acoustic mode since this mode shows very

weak softening when T_1 is approached from above. Such weak softening indicates also that frequency of the optic mode, coupled to this acoustic mode, decreases slightly. On the other hand, our recent analysis of the central peak showed very clear critical slowing down of the B -symmetry mode near T_1 .¹² This result suggests that there are at least two B -symmetry soft modes in the monoclinic phase of KMWP, which have significantly different frequencies. The higher frequency soft mode is responsible for the observed coupling with the acoustic mode, and the lower frequency soft mode, observed as the central peak, triggers the phase transition at T_1 . The presence of a few different soft modes of B -symmetry can be understood on the basis of symmetry changes. The group theoretical considerations show that there should be three B -symmetry modes, which correspond to E , B_2 , and A_2 modes of the tetragonal phase. Since the dielectric studies revealed a weak anomaly for the ϵ_{11} permittivity but a large anomaly for the ϵ_{33} permittivity,⁹ it is reasonable to assume that the lower frequency soft mode relates to the A_2 -symmetry mode in the tetragonal phase, which exhibits ionic motions mainly along the z axis. It is also worth noting that a fast decrease of the coupling strength below T_1 can be most likely attributed to a fast frequency increase of the soft mode in the triclinic phase. Brillouin results suggest also that the phase transition at T_1 is slightly first-order, because the c_{33} mode exhibits an upward shift during cooling.

Let us now consider the microscopic origin of the E -symmetry soft mode. The soft mode may correspond to both the oscillatory wave and the relaxational motion (tunneling). The oscillatory waves are observed as well-defined peaks at frequencies different from the laser frequency, whereas the relaxational modes can be often observed as quasielastic scattering (central peaks). If, however, the oscillatory wave is strongly overdamped, it does not have perceptible oscillatory features and may also be observed as a central peak.²⁹ Since strong coupling between the optic and acoustic mode is observed for KMWP in a very broad temperature range, it is clear that the frequency of the E -symmetry soft mode is similar to the frequency of the TA mode in this temperature range. The relatively long relaxation time suggests that the soft mode in KMWP can be interpreted as not a relaxational mode but rather a strongly overdamped optic mode coupled with some relaxational degrees of freedom. This result gives strong evidence that KMWP belongs to the group of materials exhibiting phase transitions which are both displacive and order-disorder in nature. We would like to emphasize that the broad temperature range of the observed coupled mode phenomenon correlates with the broad temperature range in which the central peak was observed by us previously.¹² The comparison of the elementary relaxation time obtained from the coupled mode model with the relaxation time estimated from the study of a central peak as a function of temperature (see Ref. 12) shows that these values are quite similar (3.8 and 2.7 ps for phase IV as well as 0.82 and 0.74 ps for phase V, respectively). This fact suggests that the same soft mode gives rise to the observed coupled mode phenomenon and the central peak. A very similar situation was observed in DKDP.¹⁵

The former studies of KTP and its analogs showed that the ferroelectric phase transition in this class of materials is

triggered by instability of an optic mode connected mainly with the motion of alkali metal cations.^{4,5} It was suggested that this soft mode couples with a relaxation mode of an ionic conductivity nature related to jumps of the K^+ cations from site to site.^{4,5,42} The available x-ray data for KMWP also show that the main difference between the 773 K and room-temperature structures can be observed for the positions and thermal displacement factors of potassium ions.^{10,11} It is, therefore, plausible to assume that also for KMWP disorder processes in the sublattice of potassium ions play a major role in the mechanism of the phase transitions. It seems that the primary driving force in the 632.6 K phase transition is the lattice instability induced by the relaxation mode of A_2 symmetry. Another soft mode of E -symmetry is the primary driving force leading to the 535 K phase transition. This mode is probably not a pure relaxation mode but a hybrid mode that arises due to bilinear coupling between the relaxation mode and an optic mode (mainly translation of K^+ ions). The hybrid mode in turn couples bilinearly to the c_{44} acoustic mode resulting in the observed by us coupled mode phenomenon. Since KMWP exhibits large thermal displacement factors of potassium ions and the potassium ions are situated in large cavities, interacting relatively weakly with the $[MgWO_2(PO_4)_2]^{2-}$ network, it is very likely that the hybrid mode is strongly overdamped and has low frequency in a broad temperature range. The former conductivity study showed that the largest conductivity, typical for superionic materials, is observed in phase IV.⁹ It seems therefore very likely that the observed very strong damping of the LA modes and unusually strong coupled mode features in this phase can be attributed to very low frequency of the hybrid mode in this phase due to strong coupling between the soft optic mode and the relaxation mode.

IV. CONCLUSIONS

Brillouin study revealed the presence of very strong coupling between the optic mode of E -symmetry and the c_{44} acoustic mode. The observed coupling is very unusual in the sense that it is observed in a very broad temperature range

(more than 200 K) whereas in the materials, for which a coupled mode was reported, strong coupling was observed in a narrow temperature range (less than 30 K). Moreover, the strength of this coupling changes very weakly in the stability range of phase IV. We have found that this unusual behavior may be most likely related to strong coupling of the optic mode with the relaxation mode.

It has also been shown that the phase transition at $T_4 = 632.6$ K is of second-order and mainly of order-disorder type. This phase transition is accompanied by very distinct acoustic anomalies and our results show that it can be triggered either by instability of a Brillouin zone center A_2 mode, resulting in a symmetry decrease from D_4 to C_4 , or by instability of a mode from a general point of the Brillouin zone. The ferroelastic phase transition at T_2 is induced by instability of the E -symmetry mode. This transition is strongly first-order and may be intermediate between displacive and order-disorder type. The third phase transition at 434 K is most likely slightly first-order and has both an order-disorder and displacive nature. This transition is induced by instability of the B -symmetry mode of the monoclinic phase which involves significant ionic motions along tunnels occupied by potassium ions.

We would like to stress that our results show that Brillouin studies can be a very useful tool in studies of KTP analogs. In particular, these studies can give information about relaxational and coupling phenomena in those analogs which are known to exhibit the phase transition of both displacive and order-disorder nature, for instance, germanate analogs of KTP and $KFeFPO_4$. Our results also show that it is very important to study not only LA modes, but also TA modes, in different configurations, in order to obtain information about possible coupled mode phenomena.

ACKNOWLEDGMENTS

This work was done as a part of a Poland-Japan project. M. Maćzka acknowledges Tsukuba University for support of his stay in Japan and A. Hushur for his help in Brillouin measurements.

-
- ¹G. D. Stucky, M. L. F. Phillips, and T. E. Gier, *Chem. Mater.* **1**, 492 (1989).
²J. Hellstrom, V. Pasiskevicius, F. Laurell, and H. Karlsson, *Opt. Lett.* **24**, 1233 (1999).
³V. K. Yanovskii and V. I. Voronkova, *Phys. Status Solidi A* **93**, 99 (1980).
⁴R. V. Pisarev, R. Farhi, P. Moch, and V. I. Voronkova, *J. Phys.: Condens. Matter* **2**, 7555 (1990).
⁵M. Serhane, C. Dugautier, R. Farhi, P. Moch, and R. V. Pisarev, *Ferroelectrics* **124**, 373 (1991).
⁶M. Serhane and P. Moch, *J. Phys.: Condens. Matter* **6**, 3821 (1994).
⁷C.-S. Tu, R. S. Katiyar, V. H. Schmidt, R. Guo, and A. S. Bhalla, *Phys. Rev. B* **59**, 251 (1999).
⁸E. L. Belokoneva, K. S. Knight, W. I. F. David, and B. V. Mill, *J.*

- Phys.: Condens. Matter* **9**, 3833 (1997).
⁹U. Peuchert, doctoral thesis, University of Cologne, Germany, 1995.
¹⁰U. Peuchert, L. Bohaty, and J. Schreuer, *Acta Crystallogr., Sect. C: Cryst. Struct. Commun.* **53**, 11 (1997).
¹¹U. Peuchert, L. Bohaty, and J. Schreuer, *J. Appl. Crystallogr.* **31**, 10 (1998).
¹²M. Maczka, J. Hanuza, A. Majchrowski, and S. Kojima, *Appl. Phys. Lett.* **90**, 122903 (2007).
¹³F. M. Jiang and S. Kojima, *Appl. Phys. Lett.* **77**, 1271 (2000).
¹⁴W. F. Oliver, C. A. Herbst, S. M. Lindsay, and G. H. Wolf, *Rev. Sci. Instrum.* **63**, 1884 (1992).
¹⁵R. L. Reese, I. J. Fritz, and H. Z. Cummins, *Phys. Rev. B* **7**, 4165 (1973).
¹⁶J. M. Vaughan, *Fabry-Perot Interferometer: History, Theory,*

- Practice, and Applications* (A. Hilger, Bristol, England, 1989).
- ¹⁷N. Angert, M. Tseitlin, E. Yashchin, and M. Roth, *Appl. Phys. Lett.* **67**, 1941 (1995).
- ¹⁸W. Reese and L. F. May, *Phys. Rev.* **167**, 504 (1968).
- ¹⁹H. Z. Cummins and P. E. Schoen, *Laser Handbook*, edited by F. T. Arecchi and E. O. Schultz-DuBois (North-Holland, Amsterdam, 1972).
- ²⁰H. Z. Cummins, *Light Scattering Near Phase Transitions*, edited by H. Z. Cummins and A. P. Levanyuk (North-Holland, Amsterdam, 1983).
- ²¹W. Rehwald, *Adv. Phys.* **22**, 721 (1973).
- ²²S. Yoshida, Y. Tsujimi, and T. Yagi, *Physica B* **219-220**, 596 (1996).
- ²³L. D. Landau and J. M. Khalatnikov, *Dokl. Akad. Nauk SSSR* **96**, 469 (1954).
- ²⁴M. E. Lines and A. M. Glass, *Principles and Application of Ferroelectrics and Related Materials* (Clarendon, Oxford, 1977), Chap. 8, p. 241.
- ²⁵M.-S. Zhang, T. Yagi, W. F. Oliver, and J. F. Scott, *Phys. Rev. B* **33**, 1381 (1986).
- ²⁶I. Tatsuzaki, M. Kasahara, M. Tokunaga, and H. Tanaka, *Ferroelectrics* **39**, 1049 (1981).
- ²⁷R. W. Gammon and H. Z. Cummins, *Phys. Rev. Lett.* **17**, 193 (1966).
- ²⁸P. Kuzel, P. Moch, A. Gomez-Cuevas, and V. Dvorak, *Phys. Rev. B* **49**, 6553 (1994).
- ²⁹M. Yamaguchi, M. Watanabe, K. Inoue, Y. Akishige, and T. Yagi, *Phys. Rev. Lett.* **75**, 1399 (1995).
- ³⁰M. Sawafuji, M. Tokunaga, and I. Tatsuzaki, *J. Phys. Soc. Jpn.* **47**, 1860 (1979).
- ³¹H. Tanaka and I. Tatsuzaki, *Solid State Commun.* **35**, 285 (1980).
- ³²M. Yamaguchi, M. Watanabe, Y. Akishige, K. Inoue, and T. Yagi, *Physica B* **219-220**, 647 (1996).
- ³³T. Yagi, *Ferroelectrics* **150**, 131 (1993).
- ³⁴A. M. Pugachev, S. Kojima, and A. Hushur, *Phys. Status Solidi C* **11**, 3122 (2004).
- ³⁵D. Merunka and B. Rakvin, *Solid State Commun.* **129**, 375 (2004).
- ³⁶I. P. Swainson, R. P. Hammond, J. K. Cockcroft, and R. D. Weir, *Phys. Rev. B* **66**, 174109 (2002).
- ³⁷A. Aharony, *Phys. Rev. B* **8**, 3363 (1973).
- ³⁸M. Tokunaga, *Prog. Theor. Phys.* **51**, 1002 (1974).
- ³⁹T. Yagi, M. Tokunaga, and I. Tatsuzaki, *J. Phys. Soc. Jpn.* **40**, 1659 (1976).
- ⁴⁰I. G. Siny, G. O. Andrianov, A. I. Fedoseev, V. V. Lemanov, and M. D. Volnyansky, *J. Phys.: Condens. Matter* **7**, 4283 (1995).
- ⁴¹T. Shima, M. Kasahara, P. Kaung, and Y. Yagi, *J. Phys. Soc. Jpn.* **65**, 1102 (1996).
- ⁴²B. Mohamadou, G. E. Kugel, F. Brehat, B. Wyncke, G. Marnier, and P. Simon, *J. Phys.: Condens. Matter* **3**, 9489 (1991).